Polymer Journal (2011) 43, 700–707

www.nature.com/pj

ORIGINAL ARTICLE

On the preparation of composite poly(butyl acrylate)/carbon nanotube nanoparticles by miniemulsion polymerization of butyl acrylate

Ignác Capek and Teodora Kocsisová

Miniemulsion polymerization of butyl acrylate initiated by 2,2′-azobisisobutyronitrile in the presence of carbon nanotubes (CNTs) has been investigated. The miniemulsions were stabilized by non-ionic, cationic and anionic emulsifiers. The maximal rate of polymerization (R_{pmax}) increases with the type of emulsifier in the following order: Triton X-405 (Tr) < Tween 60 (Tw) ~ dioctyl sodium sulfosuccinate (AOT) < Dowfax 2A1 (DW) ~ cetylpyridinium bromide (CPB) < cetyl trimethylammonium bromide (CTAB). R_{pmax} increases on addition of CNTs in the runs with Tw and Tr, slightly increases in the runs with CTAB, AOT and DW, and decreases in the run with CPB. Particle evolution is discussed in terms of two 'apparent' limiting cases: zero-one and pseudo-bulk kinetics. In the former case (polymer nanoparticles (PNP) approach), monomer droplets are nucleated by simple entry of radicals and transformed into polymer particles by growth events. Pseudo-bulk kinetics govern the polymerization process by the formation of radicals in the monomer phase (monomer/polymer nanoparticles (MPNP) approach).
Polymer Journal (2011) **43,** 700–707; doi:10.1038/pj.2011.50; published online 8 June 2011

Keywords: butyl acrylate; CNTs; composite; miniemulsion polymerization; nanoparticles

INTRODUCTION

Since their discovery in 1991, carbon nanotubes (CNTs) have attracted enormous attention for their fundamental behavior and potential applications.[1,2] When CNTs are introduced into an emulsion, many properties of the materials can be improved, including mechanical properties, adhesion force, aging resistance, ultraviolet resistance and surface appearance. To optimize the potential applications of CNTs, it is essential to attach suitable nanostructures or polymers to the nanotubes.[3] This renders the tubes soluble in aqueous or organic solvents, opening the possibility for further modifications through subsequent solution-based chemistry. Analogous to nanotube functionalization with carboxyl groups, the direct covalent attachment of functional moieties to their sidewalls strongly enhances the solubility of nanotubes.

Unmodified CNTs are very hydrophobic and aggregate readily. Detergents (emulsifiers) such as sodium dodecyl sulfate (SDS) are commonly used to solubilize CNTs in water.[4–6] The use of cationic emulsifiers to condense CNTs and form complexes with enhanced surfaces is well documented.[7] A common factor is that surfactants possessing longer tail groups and more unsaturated carbon–carbon bonds greatly contribute to stabilizing CNT dispersions and reducing the size of CNT agglomerates. The presence of nonionic surfactant could lead to complex micelle formation with CNTs in both aqueous and organic systems.[8] It is possible that such surfactant–nanotube interactions alter nanotube surface properties, modulating their interaction with other additives. Among them belong π–π interactions of CNT sidewalls with the aromatic compounds responsible for the formation of different complexes or aggregates.[9] In general, addition reactions to the partial carbon–carbon double bonds cause the transformation of sp^2- into sp^3-hybridized carbon atoms.[10] Zheng *et al.*[11] demonstrated that CNTs have an affinity for polymers, presumably due to hydrophobic interactions. CNTs exhibit different inhibition activities under the varied conditions of the polyreaction: the kind of monomer, solvent or initiator, because they contain fragments with characteristics of high- and low-effective inhibitors. The most active fragments of CNTs are the sites with the highest curvature (caps at the ends of nanotubes), whereas their sidewalls exhibit lower activity. Because the contribution of nanotube fragments acting as high-effective inhibitors is small, as indicated by their short induction times (up to 13 min), the deactivation concerns the primary and initiating radicals to a small degree. The macro-radicals are mostly deactivated by nanotube fragments less active than those causing the inhibition. Therefore, polymerization proceeds at a significantly slower rate than that measured in the reference process.[12,13]

Droplet nucleation is a distinct feature of miniemulsion polymerization that allows the preparation of a wide range of useful polymer and composite nanoparticles. The successful synthesis of such materials requires efficient nucleation of the monomer droplets. This can be illustrated by considering the synthesis of polymer–CNT hybrid dispersions. In this process, CNTs are dissolved in a monomer mixture

Polymer Institute, Slovak Academy of Sciences, Bratislava, Slovakia
Correspondence: Dr I Capek, Polymer Institute, Slovak Academy of Sciences, Dúbravská cesta 9, 845 41 Bratislava, Slovakia.
E-mail: upolign@savba.sk or Ignac.Capek@savba.sk
Received 9 December 2010; revised 14 March 2011; accepted 19 March 2011; published online 8 June 2011

containing a co-stabilizer and dispersed in an aqueous solution of surfactants to obtain a monomer miniemulsion. The challenge is to transform most of the droplets saturated with CNTs into polymer–CNT composite nanoparticles. This requires the nucleation of all droplets to avoid monomer transfer from droplets to active monomer/polymer particles and to minimize secondary nucleation.

The major thrust of this work is to study the effect of different emulsifiers in the presence of CNTs on miniemulsion polymerization of butyl acrylate (BuA). It has been reported that the interaction between poly(butyl acrylate) and CNTs is operative.[14] This is one reason that we chose the miniemulsion polymerization of BuA to encapsulate CNTs. We discuss the polymerization data within two limiting 'apparent' cases for monomer droplet nucleation. In the first case, each nucleated monomer droplet transforms into a polymer particle, and nucleation proceeds throughout the zero-one polymerization case (PNP). In the second case, the monomer phase or monomer droplets are saturated with oil-soluble initiator (2,2′-azobisisobutyronitrile, AIBN), and monomer droplets are transformed into monomer/polymer nanoparticles at low conversion (at conv.$_{Rpmax}$; MPNPs, pseudo-bulk polymerization).

EXPERIMENTAL PROCEDURE

Materials

After being cleaned with 10 wt% NaOH solution, commercially available BuA was purified by distillation under reduced pressure before use. Commercially available polystyrene (Sigma-Aldrich Chemie GmbH, Steinheim, Germany, M_w=2.0×10^5 g mol^{-1}) was used as the hydrophobic agent in the miniemulsion polymerization. The reagent-grade nonionic emulsifiers used were Tween 60 (Tw, Fluka, purum) and TRITON X-405 (Tr, Acros Organics, p.a., Geel, Belgium). The cationic emulsifiers used were CTAB (Lachema–Brno, purum) and CPB (Lachema–Brno, purum). The anionic emulsifiers used were AOT (Fluka, purum) and DOWFAX 2A1 (DW, Midland, Michigan, USA, purum). Emulsifiers were used as obtained without cleaning. AIBN (Acros Organics, p.a.) was used without cleaning as an initiator. Commercially available CNTs (Nanocyl s.a., Sambreville, Belgium) were used as received without pretreatment. Twice distilled water was used as a polymerization medium.

Procedures

Batch miniemulsion polymerization of BuA was carried out at 60 °C using the following recipe: 15 g distilled water; 1.5 g BuA monomer; 0.126 g AIBN; 0.015 g polystyrene (co-stabilizer); emulsifier and varied amounts of CNTs as shown in Tables 1–6. Miniemulsions were prepared by dissolving the emulsifier in water and the co-stabilizer in monomer. The oily and aqueous solutions were mixed with a mechanical agitator at 400 r.p.m. for 30 min and then by ultrasonic homogenization (Sonic Dismembrator, Model 500, Wilhington, NC, USA) for 10 min. After homogenization, miniemulsions were charged into a dilatometer.

Monomer conversion was determined by the dilatometric method.[15] Particle sizes of diluted samples (for a minimum of four different concentrations each after diluting with distilled water) were measured by the dynamic light scattering method with a Particle Sizer Model BI-90 (Brookhaven Instruments, Holtsville, NY, USA).[16] Conductivity was determined by a conductometer OK 102/1 (Radelkis, Budapest, Hungary) with a range from 0.1 μS to 0.5 S.[17] Surface tension was measured using a model K100 glass stalagmometer and tensiometer (A. KRÜSS Optronic, Hamburg, Deutschland).[18] The polymerization technique, preparation of polymer latex for size measurements, calculation of polymerization rate and estimation of particle number have been described in earlier studies.[18–21]

Local surface structures were investigated with an an Autoprobe CP research atomic force microscope operating in tapping mode. Gold-coated silicon cantilevers were used, which had a resonance frequency of 60 kHz. Cantilever tips had a high aspect ratio and asymptotic conical shape. The measurements were performed at room temperature in air. Each height and phase micrograph consisted of 256 lines, scanned at a frequency of 0.25–1.0 Hz. The background noise due to scanner-tube movement was fully subtracted from the raw data.

Size, shape and ordering of nanoparticles were studied by scanning electron microscopy. Scanning electron microscopy was performed on selected samples using a field emission scanning electron microscopy (Zeiss Gemini 1530 LEO, Oberkochen, Germany) operated at an acceleration voltage of 1–3 kV with a lateral resolution down to 1 nm. All images were taken with the secondary electron detector. The samples were investigated without staining. The working distance was 1 mm.

RESULTS AND DISCUSSION

Conversion curves

We used the oil-soluble initiator (AIBN) to accelerate the initiation of polymerization in the monomer droplets. The negatively charged surface of the CNTs was expected to interact strongly with the cationic emulsifiers and only slightly with the nonionic and anionic emusifiers. This interaction can also vary with the hydrophilic and hydrophobic properties of the emulsifiers. It was expected that the interaction between hydrophobic CNTs and hydrophobic molecules could improve the formation of hybrids and/or the incorporation of CNT fragments into the polymer particle matrix. This was thought to be correlated with the variation of kinetic and colloidal parameters of the miniemulsion polymerization with the emulsifier type.

Conversion curve shape (Figures 1–3) deviated from the S-shape typical of emulsion polymerization but was typical of miniemulsion polymerization. Conversion curves were concave downward throughout polymerization.

Figure 1 and Table 1 show that the miniemulsion polymerization of BuA reached a limiting conversion at ~15 min. In the Tw system, the limiting conversion was ~70%, whereas with Tr, the limiting conversion reached a very low value ~45%. This behavior cannot be

Table 1 Variation of kinetic and colloidal parameters with Tw and Tr (NE) in the miniemulsion polymerization of BuA, with and without CNTs

	Conv. (%)[a]			d_p *(nm)*[c]		$N_p \times 10^{-17}$ *dm*$^{-3}$[d]				*n̄/particle*[e]	
CNTs, (g)/NE	*(I)*	*(II)*	$R_{pmax} \times 10^4$ *(mol dm*$^{-3}$ *s*$^{-1}$*)*[b]	*(I)*	*(II)*	*(Ia)*	*(Ib)*	*(IIa)*	*(IIb)*	*(Ia)*	*(Ib)*
0/Tw	28.0	73.1	14.3	101	100	0.51	1.82	1.32	1.8	0.32	0.09
0/Tr	20.2	52.3	9.0	114	112	0.23	1.14	0.66	1.26	0.44	0.09
0.001/Tw	27.0	84.5	19.7	106	104	0.42	1.56	1.32	1.56	0.53	0.14
0.001/Tr	21.5	69.3	15.5	112	112	0.28	1.30	0.92	1.32	0.61	0.13

Abbreviations: BuA, butyl acrylate; CNT, carbon nanotube; conv., conversion; NE, nonionic emulsifiers.
[a]Conversion at R_{pmax} (I) and final conversion (II).
[b]Maximal rate of polymerization.
[c]Polymer particle diameter at conv.$_{Rpmax}$ (I) and at final conversion (II).
[d]Number of polymer particles (PNP) at conv.$_{Rpmax}$ (Ia) and at final conversion (IIa), and number of monomer/polymer particles (MPNP) at conv.$_{Rpmax}$ (Ib) and at final conversion (IIb).
[e](Ia) Average number of radicals per polymer particle (PNP) at conv.$_{Rpmax}$, (Ib) average number of radicals per monomer/polymer particle (MPNP) at conv.$_{Rpmax}$.

Table 2 Variation of kinetic and colloidal parameters with CPB and CTAB (CE) in the miniemulsion polymerization of BuA, with and without CNTs

	Conv. (%)[a]			d_p *(nm)*[c]		$N_p \times 10^{-17}$ *dm*$^{-3}$[d]				*n̄/particle*[e]	
CNTs(g)/CE	*(I)*	*(II)*	$R_{pmax} \times 10^4$ *(mol dm*$^{-3}$ *s*$^{-1}$*)*[b]	*(I)*	*(II)*	*(Ia)*	*(Ib)*	*(IIa)*	*(IIb)*	*(Ia)*	*(Ib)*
0/CPB	22.4	81.3	15.7	133	132	0.18	0.80	0.64	0.79	0.99	0.22
0/CTAB	29.8	72.4	20.5	103	100	0.51	1.71	1.23	1.70	0.45	0.13
0.001/CPB	29.6	58.4	13.5	163	160	0.13	0.44	0.25	0.43	1.19	0.34
0.001/CTAB	29.2	75.2	22.9	99	99	0.56	1.92	1.44	1.92	0.46	0.13

Abbreviations: BuA, butyl acrylate; CE, cationic emulsifiers; CNT, carbon nanotube; conv., conversion.
See legend to Table 1.

Table 3 Variation of kinetic and colloidal parameters with AOT and DW (AE) in miniemulsion polymerization of BuA, with and without CNTs

	Conv. (%)[a]			d_p *(nm)*[c]		$N_p \times 10^{-17}$ *dm*$^{-3}$[d]				*n̄/particle*[e]	
CNTs (g)/AE	*(I)*	*(II)*	$R_{pmax} \times 10^4$ *(mol dm*$^{-3}$ *s*$^{-1}$*)*[b]	*(I)*	*(II)*	*(Ia)*	*(Ib)*	*(IIa)*	*(IIb)*	*(Ia)*	*(Ib)*
0/AOT	35.6	77.6	14.6	119	117	0.39	1.09	0.85	1.09	0.42	0.15
0/DW	28.1	74.9	15.2	113	112	0.36	1.28	0.96	1.28	0.47	0.13
0.001/AOT	31.5	80.3	16.1	123	120	0.31	0.98	0.80	0.99	0.58	0.18
0.001/DW	33.8	77.3	16.4	178	175	0.11	0.33	0.25	0.32	1.66	0.56

Abbreviations: AE, anionic emulsifiers; BuA, butyl acrylate; CNT, carbon nanotube; conv., conversion.
See legend to Table 1.

Table 4 Kinetic parameters for emulsion polymerization of butyl acrylate

Parameter	*Numerical value*
$k_{d,AIBN}$	7.0×10^{16} $(-139805/RT)$ s^{-1}
k_p	7.37×10^5 exp $(-1157/T)$ l mol^{-1} s^{-1}
k_t	17.13×10^9 exp $(-1083/T)$ l mol^{-1} s^{-1}
$k_{fm}=k_{tr}$	2.9×10^5 exp $(-3921/T)$ l mol^{-1} s^{-1}
F	0.6
m_d,	1/1050,
[I]	0.05 mol dm^{-3}
M_p	2.35 mol dm^{-3}
D_w	1.7×10^{-5} cm^2 s^{-1}
D_c	4.1×10^{-5} cm^2 s^{-1}
D_p	8.66×10^{-7} cm^2 s^{-1}
C_w	6.4×10^{-3} mol dm^{-3}

Table 5 Variation of desorption rate coefficients with emulsifier type and nucleation approach (PNP and MPNP) in the miniemulsion polymerization of BuA[a]

	k_{des} *(cm*^{2} *s*$^{-1}$*)*				ρ_a *(M s*$^{-1}$*)*		ρ_a/ρ_i	
	$I\times10^{12}$	$I\times10^{10}$			*I*		*I*	
E type	*(1)*	*(2)*	$II\times10^{11}$	$III\times10^{12}$	*(1)*	*(2)*	*(1)*	*(2)*
Tw	4.46	0.93	10.99	8.18	0.24	0.06	1.56	5.55
Tr	1.82	2.21	10.99	8.22	0.05	0.14	1.13	6.25
CPB	—	0.43	10.99	8.26	—	0.13	—	2.27
CTAB	0.62	0.45	10.99	8.18	0.02	0.05	1.09	3.85
DW	0.57	0.72	10.99	8.21	0.03	0.08	1.06	3.85
AOT	1.48	0.67	10.99	8.23	0.05	0.1	1.19	3.33

[a]I, Ugelstadt/O'Tool model, (1) polymer particles and (2) monomer/polymer particles; II, Nomura model; III, Gilbert model.

Table 6 Variation of desorption rate coefficients with emulsifier type and nucleation approach (PNP and MPNP) in the miniemulsion polymerization of BuA, in the presence of CNTs[a]

	k_{des} *(cm*^{2} *s*$^{-1}$*)*				ρ_a *(M.s*$^{-1}$*)*		ρ_a/ρ_i	
	$I\times10^{15}$	$I\times10^{10}$			I		*I*	
E type	*(1)*	*(2)*	$II\times10^{11}$	$III\times10^{12}$	*(1)*	*(2)*	*(1)*	*(2)*
Tw	0.1	0.44	10.99	8.19	0.02	0.05	1.00	3.57
Triton	0.1	0.69	10.99	8.21	0.03	0.08	1.00	3.85
CPB	0.01	0.28	10.99	8.29	0.34	0.28	1.01	1.47
CTAB	4.09	0.37	10.99	8.17	0.01	0.04	1.08	3.85
DW	0.07	0.004	10.99	8.31	0.43	0.33	1.00	1.00
AOT	0.27	0.50	10.99	8.24	0.05	0.10	1.00	2.78

[a]I, Ugelstadt/O'Tool model, (1) polymer particles and (2) monomer/polymer particles; II, Nomura model; III, Gilbert model.

ascribed to the consumption of initiator because the half time of AIBN is much longer than 10 h at 60 °C.[22] The appearance of the limiting conversion can theoretically be explained by a low monomer concentration at reaction loci, immobilization of AIBN and emulsifier in the polymer particle matrix, deactivation of radicals and/or low radical entry efficiency. The low T_g for PolyBuA disfavors the effect of the glassy state on the polymerization process under the given reaction conditions. The high oil solubility of both emulsifiers (Tw and Tr) could be one of the parameters responsible for the retardation of polymerization via chain transfer events.

Retardation or inhibition of polymerization of some alkyl acrylates is observed in the presence of CNTs.[12] Figure 1 indicates that this was not true for the present miniemulsion polymerizations of BuA. On the contrary, CNTs increased the final conversion in both systems. In the Tw system, conversion strongly increased from 45 to 65%. In the Tr system, conversion increased from 70 to 85% (in 15 min).

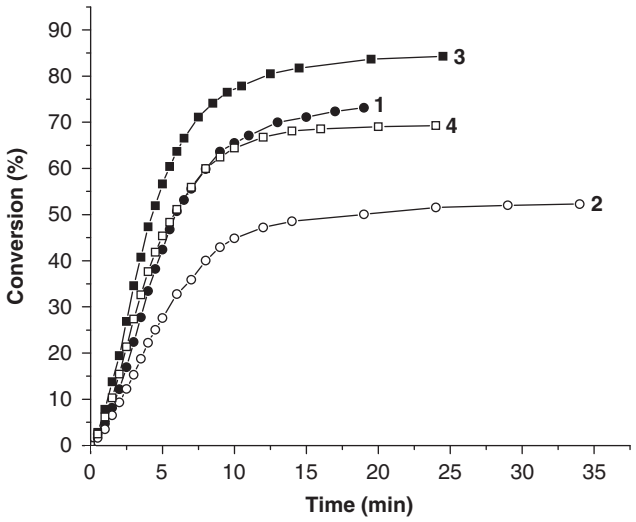

Figure 1 Variation of monomer conversion with reaction time in the miniemulsion polymerization of butyl acrylate stabilized by Tw or Tr, with and without carbon nanotubes (CNTs). (1) 0.2 g Tw, (2) 0.41 g Tr, (3) 0.2 g Tw + 0.001 g CNTs and (4) 0.41 g Tr + 0.001 g CNTs.

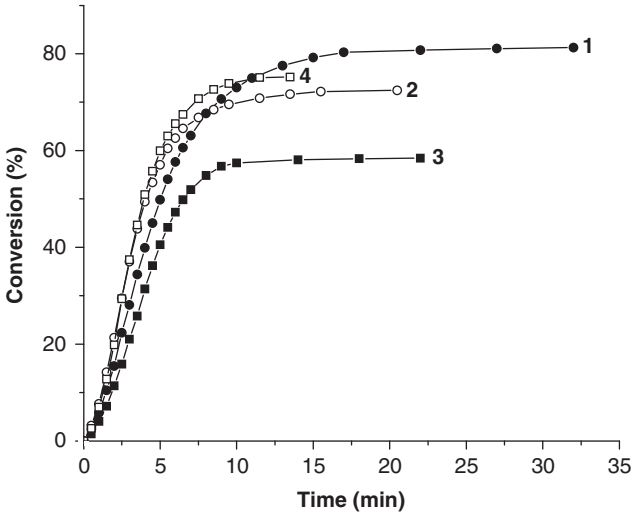

Figure 2 Variation of monomer conversion with reaction time in the miniemulsion polymerization of butyl acrylate stabilized by CPB or CTAB, with and without carbon nanotubes (CNTs). (1) 0.06 g CPB, (2) 0.06 g CTAB, (3) 0.06 g CPB + 0.001 g CNTs and (4) 0.06 g CTAB + 0.001 g CNTs.

The interaction of CNTs with poly(ethylene oxide) chains seems to favor growth events.[23] Furthermore, the interaction of CNTs (π-conjugated system) with AIBN molecules might increase the decomposition of AIBN and the concentration of radicals in the system.[9] A monomer/polymer particle saturated with AIBN molecules can act as a cage that decreases the concentration of primary radicals. The presence of CNTs might form a barrier against the biradical termination of radicals and might favor the escape of radicals from the cage. Indeed, in both cases, the number of particles and the average number of radicals per particle increased (Table 1). We cannot exclude the contribution of 'active' CNT fragments generated by the ultrasound in the pretreatment period to the total radical concentration.[12]

In the CTAB system (Figure 2 and Table 2), the limiting conversion increased upon addition of CNTs, from 70 to 80%. By contrast, the limiting conversion strongly decreased in the CPB system, from 80 to 55%. The increase in conversion has already been explained by the increased concentration of particles and radicals and increased stability of polymer particles. On the contrary, the decrease in the limiting conversion can be attributed to lower concentrations of both radicals and particles and lower colloidal stability. Cationic CPBs are known to interact with the negatively charged sidewalls of CNTs via both electrostatics (charge) and π-electrons to generate a CPB/CNT associate.[24,25] This complex within the monomer/polymer particle might react with radicals and decrease the level of radicals. That the ratio [CPB]/CNTs was 9.0 mol g^{-1} indicates that most of the CNTs should have been part of these CPB/CNT associates. Thus, encapsulated CPB/CNT associates may act as radical scavengers and depress growth events.[12,13]

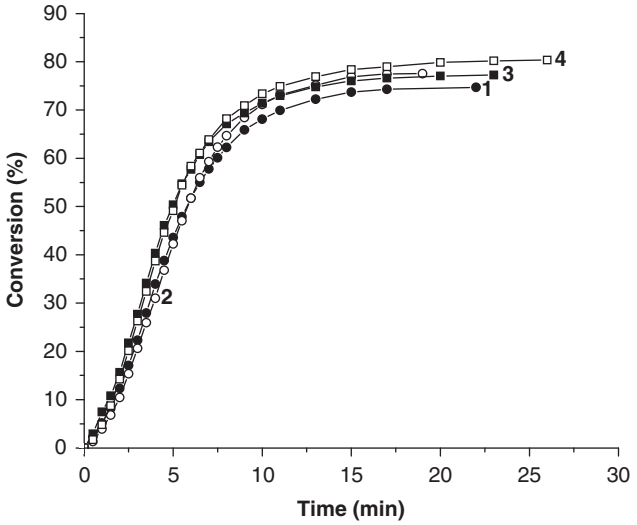

Figure 3 Variation of monomer conversion with reaction time in the miniemulsion polymerization of butyl acrylate stabilized by DW or AOT, with and without carbon nanotubes (CNTs). (1) 0.15 g DW, (2) 0.07 g AOT, (3) 0.15 g DW + 0.001 g CNTs and (4) 0.07 g AOT + 0.001 g CNTs.

Miniemulsion polymerizations stabilized by anionic emulsifiers (AOT and DW), with and without CNTs, were also studied, and the results are shown in Figure 3 and Table 3. Limiting conversions and the shapes of conversion curves were similar for both AOT and DW. Furthermore, a slight increase in conversion was observed for both AOT and DW upon addition of CNTs. This behavior supports the idea that either negatively charged CNTs do not interact with anionic emulsifier molecules or the interaction is weak, and therefore the polymerization is not influenced.

Rate of polymerization

Variation in the rate of polymerization with conversion and type of emulsifier is illustrated in Figures 4–6. Neither the three rate intervals (with a distinct Interval 2) typical for emulsion polymerization nor the four rate intervals typical for miniemulsion polymerization of styrene appeared. The dependence of conversion on polymerization rate is described by a curve with two rate intervals and a maximum rate (R_{pmax}) at a particular conversion ($conv._{Rpmax}$).

The shift of R_{pmax} to a higher conversion can be ascribed to the prolonged nucleation period and the generation of a higher concentration of polymer particles (Table 1). The pronounced increase in the rate of polymerization up to $conv._{Rpmax}$ can be explained by the increased particle concentration and the gel effect. The gel effect in

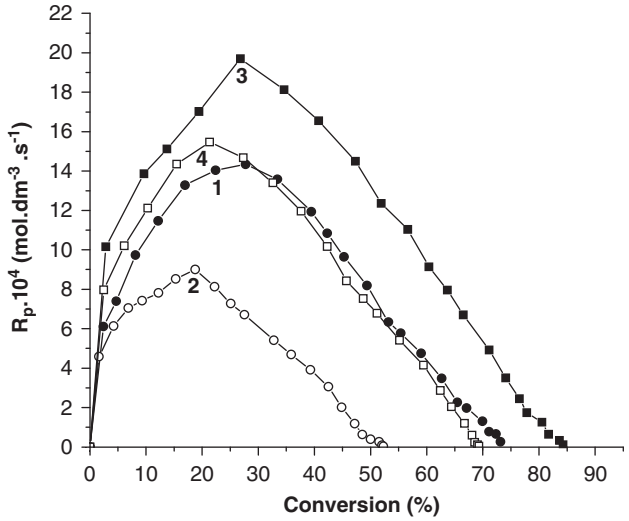

Figure 4 Dependence of polymerization rate on monomer conversion and nonionic emulsifier (Tw and Tr) type in the miniemulsion polymerization of butyl acrylate, with and without carbon nanotubes (CNTs). (1) 0.2 g Tw, (2) 0.41 g Tr, (3) 0.2 g Tw + 0.001 g CNTs and (4) 0.41 g Tr + 0.001 g CNTs.

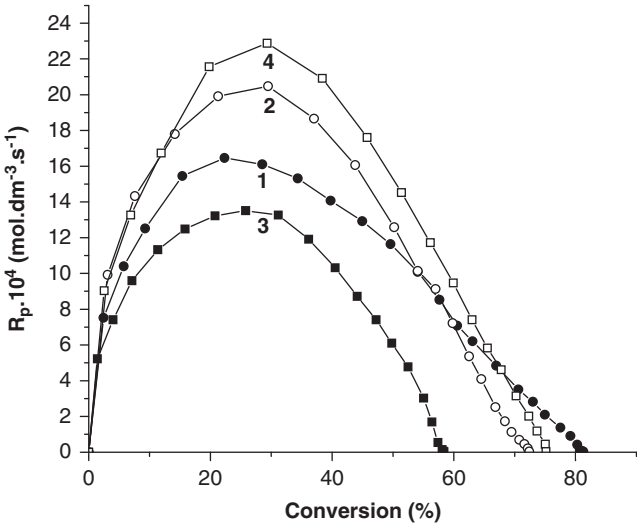

Figure 5 Dependence of polymerization rate on monomer conversion and cationic emulsifier (CPB and CTAB) type in the miniemulsion polymerization of butyl acrylate, with and without carbon nanotubes (CNTs). (1) 0.06 g CPB, (2) 0.06 g CTAB, (3) 0.06 g CPB + 0.001 g CNTs and (4) 0.06 g CTAB + 0.001 g CNTs.

bulk polymerization of alkyl (meth)acrylates is located at approximately 20–30% conversion.[26] The abrupt decrease in polymerization rate beyond approximately 30–50% conversion can be explained by the decrease of monomer concentration at reaction loci and the increased deactivation of radicals via immobilization of initiator and increased contribution of pseudo-bulk kinetics.

Polymerization of BuA proceeded much faster with Tw than with Tr. This difference can be attributed to the larger number of polymer particles formed in the Tw run. Addition of CNTs increased R_{pmax} by a factor of 1.4 with Tw and a factor of 1.7 with Tr. The number of polymer particles increased in the Tr/CNTs run but did not change in the Tw/CNTs run.

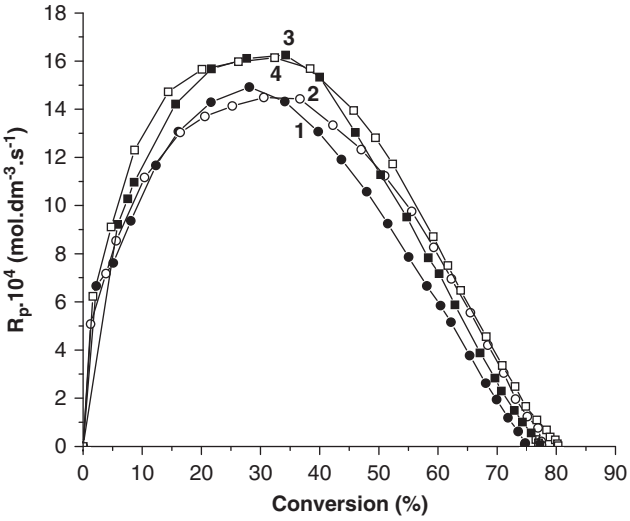

Figure 6 Dependence of polymerization rate on monomer conversion and anionic emulsifier (DW and AOT) type in the miniemulsion polymerization of butyl acrylate, with and without carbon nanotubes (CNTs). (1) 0.15 g DW, (2) 0.07 g AOT, (3) 0.15 g DW + 0.001 g CNTs and (4) 0.07 g AOT + 0.001 g CNTs.

In the Tw and Tr runs, R_{pmax} was located at a conversion of approximately 20–30%; that is, at this conversion, one-third of the monomer is converted to polymer. We discuss the experimental data in two limiting 'apparent' cases for particle evolution. (1) Each nucleated droplet is converted to a polymer particle; that is, in the present case, approximately one-third of the monomer droplets are converted to polymer particles at conv.$_{Rpmax}$, and the rest of the monomer is located in inactive monomer droplets (Table 1, PNP approach). (2) The nucleation starts in monomer droplets, and monomer droplets are continuously converting to monomer–polymer particles (Table 1, MPNP approach). For example, Ia in Table 1 denotes the number of polymer particles (the rest of the monomer is in free unreacted droplets), and Ib denotes the monomer/polymer particles (monomer droplets and polymer particles are not present) (Table 1). According to the first approach, the number of polymer particles increases during polymerization. The second approach suggests that the number of monomer/polymer particles (monomer-saturated polymer particles) reaches a maximal and constant value at low conversion. In this MPNP approach, the gel effect appears at medium conversions, and therefore a strong increase in R_p (R_{pmax}) is observed.

The number of particles (Tables 1–2) was used to estimate the average number of radicals per particle ($\bar{n}$) at convR_{pmax}. The estimated number of radicals per particle for polymer particles ($\bar{n} \leqslant 0.5$, PNP) was several times larger than the $\bar{n}$ for monomer/polymer particles ($\bar{n} \leqslant 0.1$, MPNP). The real value of $\bar{n}$ is assumed to be somewhere between these two limiting cases. The average number of radicals per particle estimated for the medium conversion $\bar{n}$ (0.1–0.5) indicates the compartmentalization of reaction loci ($\bar{n} \leqslant 0.5$, PNP) and increased termination of radicals.

Variation of polymerization rate with conversion and cationic emulsifier type is illustrated in Figure 5 and Table 2. Maximal rate of polymerization (R_{pmax}) without CNTs increased in the following order: Tr < Tw ~ AOT < DW ~ CPB < CTAB. These data show that the most active polymerizations were those involving cationic emulsifiers. The dependence of conversion on polymerization rate for CPB and CTAB is described by a curve with two rate intervals and a maximum

rate at conversions of 25 and 30%, respectively. The miniemulsion polymerization with CTAB was faster than that with CPB. The difference in R_{pmax} can be attributed to the larger number of polymer particles in the CTAB run. Furthermore, $\bar{n}$ was close to 0.5 for CTAB and to 1.0 for CPB. Thus, this difference can also be attributed to the compartmentalization of reaction loci for CTAB, while the gel effect (pseudo-bulk kinetics) governs polymerization with CPB.

The addition of CNTs increased R_{pmax} by a factor of 1.1 with CTAB. By contrast, R_{pmax} decreased by a factor of 0.86 with CPB. Similar trends were observed for the number of particles. Thus, the number of polymer particles increased in the CTAB/CNTs run, but decreased in the CPB/CNTs run. Zero-one kinetics ($\bar{n} \leqslant 0.5$) is assumed to govern polymerization in the CTAB/CNTs system. By contrast, the increased contribution of pseudo-bulk kinetics leads to $\bar{n} \sim 1.0$ in the CPB/CNTs system.

Variation of the polymerization rate with conversion and anionic emulsifier type is illustrated in Figure 6 and Table 3. The dependence of conversion on polymerization rate for both AOT and DW is described by a curve with two rate intervals and a maximum rate at 25 and 35% conversion, respectively. The maximal rates of polymerization, the numbers of polymer particles and the numbers of radicals per particle were similar for both runs. The miniemulsion polymerizations with AOT and DW were both governed by zero-one kinetics for the PNP approach ($\bar{n} \leqslant 0.5$). For the MPNP approach, $\bar{n} \sim 0.1$ was obtained. The addition of CNTs increased $\bar{n}$, and that increase was much more pronounced in the DW/CNTs run. The number of polymer particles decreased upon addition of CNTs, and that decrease was much more pronounced with DW.

Desorption rate constants

Miniemulsion polymerization of BuA under the conditions described led to the production of relatively fine dispersions. This fact might favor the effect of desorption of monomer radicals on the overall polymerization kinetics. The specific desorption rate constants k'_{des} ($cm^2\,s^{-1}$) and k_{des} (s^{-1}) were calculated using three different models: the Ugelstadt/O'Tool approach (I), the Nomura model (II) and the Gilbert model (III).[27–31] The constants were calculated as described in our previous papers[32] using the data summarized in Tables 1–3 and the literature data and constants in Table 4.[33–36] The calculated exit rate constants k'_{des} ($cm^2\,s^{-1}$) and radical entry rates ρ_a (Ms^{-1}) are shown in Tables 5 and 6.

According to the Ugelstadt/O'Tool model, the k'_{des} values for the monomer-saturated particles (MPNPs) are approximately 1–2 orders of magnitude larger than those for the polymer particles (PNPs). The chain transfer to monomer and transport of monomer radicals from the particle to the continuous phase are governed by the monomer level in the monomer/polymer particles. The radical desorption rate coefficient decreases with conversion (from MPNP to PNP).

The rate coefficient of desorption, k'_{des} increased from the runs with ionic emulsifiers to those with nonionic, and the lowest k'_{des} values were observed in the runs with cationic emulsifier. The exit rate coefficient was reported to decrease with the alkyl chain length of the stabilizer on the particle surface.[37] The exit of radicals is a rather complex function of the charge and hairiness of the particle surface. Consider both effects on the two non-ionic emulsifiers Tw and Tr. Tw has 20 ethylene oxide units, whereas Tr has 40 ethylene oxide units. Thus, the particle hairiness and partial negative charge are larger in Tr. Under these conditions, the radical desorption should be more pronounced with Tw. However, the reverse was true. A larger stearoyl group in Tw made the particle shell more compact, which somehow disfavored radical desorption, whereas the octyl group structure in Tr did not form a barrier against radical desorption in the Tr runs. Similar k'_{des} values were observed in the anionics AOT and DW. The bis(2-ethylhexyl) and dodecylbenzene groups had activity similar to that of the desorption events. Desorption of radicals was more suppressed in cationics CTAB and CPB. Cetyltrimethylammonium and cetylpyridinium groups probably formed a barrier to exiting radicals, both through the bulkiness and through the positive charge of both emulsifiers. Thus, the fate of monomeric radicals in monomer/polymer particles is a complex function of both the charge (structure) of the particle shell and the particle core size.

In the presence of CNTs, k'_{des} values for MPNPs were $\sim$3 orders of magnitude larger than those for PNPs. The presence of monomer is the rate-determining step for desorption of monomer radicals. The presence of CNTs decreased the rate coefficient of radical desorption in the particles. Furthermore, variation of the exit rate coefficient k'_{des} with emulsifier charge was not so distinct for the runs with CNTs as it was for the runs without CNTs. Thus, the presence of CNTs in the polymer particles somehow influenced the radical flux. The values of k'_{des} were independent of particle size for dispersions with a size around 100 nm. According to the Nomura and Gilbert models, the values of k'_{des} were independent of emulsifier type and nucleation mode. Those models did not show any effect of CNTs, type of emulsifier or nucleation mode on the fate of radicals in the present polymerization system.

The variation of radical entry rate (ρ_a) with emulsifier type and particle nucleation mode for experiments without CNTs is shown in Table 5. The radical entry rates were somewhat larger for monomer/polymer particles (except for Tw). This slight increase can be attributed to the higher desorption rate of monomeric radicals and radical fragments of initiator (AIBN) from the monomer–polymer particles and their re-entry into other nanoparticles. We should keep in mind that the hydrophobic primary radicals derived from AIBN can also exit particles and obey first- or second-order loss mechanisms. We expect that desorbed hydrophobic radicals in the aqueous phase will be preferentially adsorbed by neighboring hydrophobic particles, and therefore the second-order loss mechanism should be preferred. We speculate that the interaction between positively charged particle surfaces (saturated with CTAB and CPB) will concentrate the radicals at the particle surface zone, where they can take part in initiation or termination. One can expect the opposite for electrostatically stabilized particles (with DW and AOT).

The ratio ρ_a/ρ_i reached values slightly above 1.0 for PNP and much above 1.0 for MPNP. Second-order radical loss kinetics might be responsible for the increase in ρ_a/ρ_i, which was much more pronounced in MPNP runs; that is, desorbed monomeric radicals re-enter other particles to either propagate or terminate.

The presence of CNTs (Table 6) decreases ρ_a, and ρ_a becomes independent of nucleation mode (PNP or MPNP). Cationic emulsifiers condense CNTs and form complexes and dense particle corona.[7] We speculate that the dense particle surface shell acts as a barrier for entering radicals. The formation of strong complex CNT/CPBs via π–π electrons probably makes denser particle shells. Poly(ethylene glycol) shows a preferential attraction to negatively charged CNT surfaces,[38] and the dense corona of CNT/Tw or CNT/Tr acts as a barrier for radicals. This might not be true for the anionics, where the interaction between DW and AOT with CNTs is weak. Addition of CNTs slightly decreased ρ_a/ρ_i. Thus, it reached 1.0 for PNP and was several times larger for MPNP. Desorbed monomeric radicals re-enter particles to either propagate or terminate. The ratio ρ_a/ρ_i is larger for nonionics than for ionics.

Characterization of polymer latexes

The surface tension (γ) and conductance (κ) of polymer latexes were measured for characterization of polymer latexes.

The surface tension (γ) for characterization of polymer latexes without CNTs varied with emulsifier type as follows:

$$\gamma(\mathrm{mN\,m^{-1}}):\ 7.2\,(\mathrm{CTAB}) < 18.3\,(\mathrm{CPB}) < 35.8\,(\mathrm{AOT}) < 37.1\,(\mathrm{Tw}) < 41.0\,(\mathrm{Tr\ and\ DW}).$$

Upon application of CNTs, the surface tension of polymer latexes slightly changed.

$$\gamma\,(\mathrm{mN\,m^{-1}}):\ 7.6\,(\mathrm{CTAB}) < 20.9\,(\mathrm{CPB}) < 31.1\,(\mathrm{AOT}) < 36.1(\mathrm{Tw}) < 37.9\,(\mathrm{Tr}) < 39.7\,(\mathrm{DW}).$$

This might indicate that CNTs are encapsulated in the polymer particles.

Conductance (κ) for characterization of the final polymer dispersion increases with the emulsifier type as follows.

$$\kappa\,(\mu\mathrm{S}):\ 270\,(\mathrm{Tw\ and\ Tr}) < 300\,(\mathrm{DW}) < 420\,(\mathrm{CPB}) < 550\,(\mathrm{CTAB}) < 650\,(\mathrm{AOT}).$$

As expected, the conductance increased from nonionic to anionic emulsifiers. Thus, the lowest conductance was observed in sterically stabilized latexes (Tw and Tr). The high conductance in the AOT run indicates the presence of free emulsifier molecules in the continuous phase and insufficient adsorption of emulsifier molecules on the particle surface. Addition of CNTs led to the following dependence:

$$\kappa\,(\mu\mathrm{S}):\ 121(\mathrm{Tr}) < 209(\mathrm{DW}) < 260(\mathrm{TW}) < 380(\mathrm{CPB}) < 550(\mathrm{CTAB}) < 710(\mathrm{AOT}).$$

The decrease in conductance can be attributed to the hydrophobic activity of CNTs, which decreases the solubility of emulsifier molecules in the aqueous phase (increases the oil solubility of emulsifier/CNTs associates).

Poly(butyl acrylate) nanoparticles are very soft and sticky, which is why we did not get measurements for individual nanoparticles with scanning electron microscopy or transmission electron microscopy but observed aggregates with strongly deformed particles. Atomic force microscope measurements showed that the surfaces of nanoparticles with and without CNTs were the same. This indicated that the CNTs were encapsulated within the poly(butyl acrylate).

CONCLUSIONS

This report discusses the effect of multiwall CNTs on the kinetics of miniemulsion polymerization of BuA initiated by AIBN. The maximal rate (R_{pmax}) of polymerization increased with emulsifier type in the following order: $\mathrm{Tr} < \mathrm{Tw} \sim \mathrm{AOT} < \mathrm{DW} \sim \mathrm{CPB} < \mathrm{CTAB}$. R_{pmax} strongly increased with CNTs in the runs with Tw and Tr, slightly increased in the runs with CTAB, AOT and DW and decreased with CPB. Here, monomer conversion followed the overall conversion of the reaction system. According to the first approach (PNP), the number of polymer particles increased during polymerization and R_{pmax} was a synergistic contribution of the increased number of reaction loci. The second approach (MPNP) suggested that R_{pmax} was the synergistic contribution of the number of monomer/polymer particles (monomer-saturated polymer particles) and gel effect. The number of reaction loci (monomer/polymer particles) was approximately constant during the polymerization. Because of the hydrophobic nature of CNTs, the hydrophobic chains of surfactants anchor on the surface of CNTs. During homogenization of the reaction mixture, the BuA monomer preferentially partitioned between the interior of emulsifier/CNTs associates and emulsifier molecules located at the droplet surface. Radicals generated by the decomposition of the initiator started polymerization in the monomer droplets saturated with CNTs. The results show that CTAB is a very efficient stabilizer for the formation and stabilization of polymer particles. The strong interaction of CTAB with CNTs probably decreases the retardation activity of CNTs. The rest of the emulsifiers with negative charge (AOT) or partially negative charge are situated between the CTAB and CPB runs; that is, they do not interact with CNTs or the interaction is very weak, and therefore they do not influence the polymerization process.

ACKNOWLEDGEMENTS

This research is supported by VEGA project nos. 2/0037/10 and 2/0160/10, APVV projects nos. 0362-07 and 0030-07 and the project implementation Centre of the Applied Nanoparticle Research, ITMS code 26240220011, supported by the Research & Development Operational Programme funded by the ERDF. We thank Ms Anna Kmetikova for experimental assistance in the preparation of polymer latexes.

1 Lijima, S. Helical microtubules of graphitic carbon. *Nature* **354,** 56–58 (1991).
2 Rotkin, S. V. & Zharov, I. Nanotube light-controlled electronic switch. *Int. J. Nanosci.* **1,** 347–355 (2002).
3 Jiang, K., Eitan, A., Schadler, L. S., Ajayan, P. M., Siegel, R. W., Grobert, N., Mayne, M., Reyes-Reyes, M., Terrones, H. & Terrones, M. Noncovalent functionalization of graphite and carbon nanotubes with polymer multilayers and gold nanoparticles. *Nano. Lett.* **3,** 275–277 (2003).
4 Chattopadhyay, D., Galeska, I. & Papadimitrakopoulos, F. A route for bulk separation of semiconducting from metallic single wall carbon nanotubes. *J. Am. Chem. Soc.* **125,** 3370–3375 (2003).
5 Yurekli, K., Mitchell, C. A. & Krishnamoorti, R. Small-angle neutron scattering from surfactant-assisted aqueous dispersions of carbon nanotubes. *J. Am. Chem. Soc.* **126,** 9902–9903 (2004).
6 Poulin, P., Vigolo, B. & Launois, P. Films and fibers of oriented single wall nanotubes. *Carbon* **40,** 1741–1749 (2002).
7 Star, A., Liu, Y., Grant, K., Ridvan, L., Stoddart, J. F., Steuerman, D. W., Diehl, M. R., Boukai, A. & Heath, J. R. Noncovalent side-wall functionalization of single-walled carbon nanotubes. *Macromolecules* **36,** 553–560 (2003).
8 Moore, V. C., Strano, M. S., Haroz, E. K., Hauge, R. H. & Smalley, R. E. Individually suspended single–walled carbon nanotubes in various surfactants. *Nano. Lett.* **3,** 1379–1382 (2003).
9 Chen, R. J., Zhang, Y., Wang, D. & Dai, H. Noncovalent sidewall functionalization of single-walled carbon nanotubes for protein immobilization. *J. Am. Chem. Soc.* **123,** 3838–3839 (2001).
10 Hu, H., Bhowmik, P., Zhao, B., Hamon, M. A., Itkis, M. E. & Haddon, R. C. Determination of the acidic sites of purified single-walled carbon nanotubes by acid-base titration. *Chem. Phys. Lett.* **345,** 25–28 (2001).
11 Zheng, M., Jagota, A., Semke, E. D., Diner, B. A., McLean, R. S., Lustig, S. R., Richardson, R. E. & Tassi, N. G. DNA-assisted dispersion and separation of carbon nanotubes. *Nat. Mater.* **2,** 338–342 (2003).
12 Onderko, K., Pabin-Szafko, B. & Szafko, J. Poly (methyl methacrylate)/carbon nanotubes composites. *Karbo* **49,** 175–181 (2004).
13 Pabin–Szafko, B., Wisniewska, E. & Szafko, J. Carbon nanotubes and fullerene in the solution polymerisation of acrylonitrile. *Eur. Polym. J.* **42,** 1516–1520 (2006).
14 Xia, H. & Qiu, G. Polymer-encapsulated carbon nanotubes prepared through ultrasonically initiated *in situ* emulsion polymerization. *Chem. Mater.* **15,** 3879–3886 (2003).
15 Fialova, L., Capek, I., Ianchis, R., Corobea, M. C., Donescu, D. & Berek, D. Kinetics of styrene and butyl acrylate polymerization in anionic microemulsions in presence of layered silicates. *Polym. J.* **160,** 1–8 (2007).
16 Menom, M., Andriotis, A. N. & Froudakis, G. E. Curvature dependence of the metal catalyst atom interaction with carbon nanotubes walls. *Chem. Phys. Lett.* **320,** 425–434 (1998).
17 Yakobson, B. I. & Brabec, C. J. Bernholc, nanomechanics of carbon tubes: instabilities beyond linear response. *J. Phys. Rev. Lett.* **76,** 2511–2514 (1996).
18 Potisk, P. & Capek, I. Microemulsion polymerization of butyl acrylate 1. Effect of initiator type and concentration. *Angew. Makromol. Chemie.* **222,** 125–146 (1994).
19 Capek, I. Emulsion copolymerization of acrylonitrile and butyl acrylate, 10. Effect of 1,1-diphenyl-2-picrylhydrazyl on the polymerization process. *Makromol. Chem.* **190,** 789–796 (1989).
20 Capek, I. & Potisk, P. Microemulsion and emulsion polymerization of butyl acrylate -I. Effect of the initiator type and temperature. *Eur. Polym. J.* **31,** 1269–1277 (1995).

21 Reimers, J. & Schork, F. J. Predominant droplet nucleation in emulsion polymerization. *J. Appl. Polym. Sci.* **60,** 251–262 (1996).
22 Brandrup, J. & Immergut, E. H. *Polymer Handbook*. 3rd edn., (John Willey and Sons Publishers, New York, 1989).
23 Tadros, T. F. & Vincent, B. Influence of temperature and electrolytes on the adsorption of poly (ethylene oxide)-poly(propylene oxide) block copolymer on polystyrene latex and on the stability of the polymer-coated particles. *J. Phys. Chem.* **84,** 1575–1580 (1980).
24 Jiang, L. Q., Gao, L. & Sun, J. Production of aqueous colloidal dispersions of carbon nanotubes. *J. Colloid Interface Sci.* **260,** 89–94 (2003).
25 Lu, K. L., Lago, R. M., Chen, Y. K., Green, M. L., Harris, P. J. & Tsang, S. C. Mechanical damage of carbon nanotubes by ultrasound. *Carbon* **34,** 814–816 (1996).
26 Dionisio, J., Mahabadi, H. K. & O'Driscoll, K. F. High-conversion polymerization. IV. A definition of the onset of the gel effect. *J. Polym. Sci. Polym. Chem. Ed.* **17,** 1891–1900 (1979).
27 Nomura, M. *Emulsion Polymerization*. (ed. Piirma, I.) (Academic Press, London, 1985).
28 Nomura, M. & Harada, M. Rate coefficient for radical desorption in emulsion polymerization. *J. Appl. Polym. Sci.* **26,** 17–26 (1981).
29 Nomura, M., Harada, M., Nakagawara, K., Eguchi, W. & Nagata, S. The role of polymer particles in the emulsion polymerization of vinyl acetate. *J. Chem. Eng. Jpn.* **4,** 160–166 (1971).
30 Ugelstad, J., Mork, P. C. & Aassen, J. O. A kinetic investigation of the emulsion polymerisation of vinyl chloride. *J. Polym. Sci.* **5,** 2281–2288 (1967).
31 Toole, J. I. Kinetics of emulsion polymerization. *J. Appl. Polym. Sci.* **9,** 1291–1297 (1965).
32 Capek, I. On the hybride inverse-emulsion polymerization of acrylamide. *Polym. Plast Technol. Eng.* **44,** 539–555 (2005).
33 Yildiz, U., Capek, I., Berek, D., Sarov, Y. & Rangelow, I. W. Inverse microemulsion copolymerization of butyl acrylate and acrylamide: kinetics, colloidal parameters and some model applications. *Polym. Int.* **56,** 364–370 (2007).
34 Ginsburger, E., Pla, F., Fonteix, C., Hoppe, S., Massebeuf, S., Hobbes, P. & Swaels, P. Modelling and simulation of batch and semi-batch emulsion copolymerization of styrene and butyl acrylate. *Chem. Eng. Sci.* **58,** 4493–4514 (2003).
35 Coen, E. M., Peach, S., Morrison, B. & Gilbert, R. G. First-principles calculation of particle formation in emulsion polymerization: pseudo-bulk systems. *Polymer* **45,** 3595–3608 (2004).
36 Jasso, C. F., Valdéz, J., Pérez, J. H. & Laguna, O. Analysis of butyl acrylate diffusion in a glassy polystyrene matrix to predict gradient structure. *J. Appl. Polym. Sci.* **80,** 1343–1348 (2001).
37 Thickett, S. C. & Gilbert, R. G. Rate-controlling events for radical exit in electrosterically stabilized emulsion polymerization systems. *Macromolecules* **39,** 2081–2091 (2006).
38 Vaisman, L., Marom, G. & Wagner, H. D. Dispersions of surface-modified carbon nanotubes in water-soluble and water-insoluble polymers. *Adv. Funct. Mater.* **16,** 357–363 (2006).